

Multi-modality Meets Re-learning: Mitigating Negative Transfer in Sequential Recommendation

Bo Peng, Srinivasan Parthasarathy, *Fellow, IEEE*, and Xia Ning*, *Member, IEEE*

Abstract—Learning effective recommendation models from sparse user interactions represents a fundamental challenge in developing sequential recommendation methods. Recently, pre-training-based methods have been developed to tackle this challenge. Though promising, in this paper, we show that existing methods suffer from the notorious negative transfer issue, where the model adapted from the pre-trained model results in worse performance compared to the model learned from scratch in the task of interest (i.e., target task). To address this issue, we develop a method, denoted as ANT, for transferable sequential recommendation. ANT mitigates negative transfer by 1) incorporating multi-modality item information, including item texts, images and prices, to effectively learn more transferable knowledge from related tasks (i.e., auxiliary tasks); and 2) better capturing task-specific knowledge in the target task using a re-learning-based adaptation strategy. We evaluate ANT against eight state-of-the-art baseline methods on five target tasks. Our experimental results demonstrate that ANT does not suffer from the negative transfer issue on any of the target tasks. The results also demonstrate that ANT substantially outperforms baseline methods in the target tasks with an improvement of as much as 15.2%. Our analysis highlights the superior effectiveness of our re-learning-based strategy compared to fine-tuning on the target tasks.

Index Terms—Recommender System, Sequential Recommendation, Transferable Recommendation



1 INTRODUCTION

SEQUENTIAL recommendation aims to leverage users' historical interactions to identify and recommend the next item of their interest. Due to the explosion in the number of available items, it has become indispensable in various applications such as online retail [1] and video streaming [2], drawing increasing attention from the research community. A fundamental challenge in developing modern sequential recommendation methods is to learn effective recommendation models from the sparse user interaction data in the task of interest, referred to as the target task. Recently, pre-training-based recommendation methods [3], [4] have been developed to tackle this challenge. These methods learn transferable knowledge from the rich interaction data in other related tasks, referred to as auxiliary tasks, via pre-training, and transfer the learned knowledge to improve recommendations for the target task.

To enable an effective transfer learning in the target task, two significant challenges need to be addressed: 1) learning transferable knowledge from auxiliary tasks applicable and beneficial for recommendations in the target task; and 2)

capturing task-specific knowledge in the target task. Current methods [3], [4] primarily learn transferable knowledge using item texts. However, as will be demonstrated in our analysis (Section 6.3), item texts in auxiliary tasks and the target task could exhibit remarkable differences in terms of wording, style and vocabulary. Consequently, limited transferable knowledge could be learned from item texts. In addition, existing methods [3] learn the task-specific knowledge in the target task via fine-tuning. However, starting from parameters pre-trained on auxiliary tasks, the fine-tuned models may struggle to capture the task-specific knowledge in the target task since the target task could be considerably different from the auxiliary ones.

Due to the above limitations, as will be shown in our analysis (Section 6.2), current methods could suffer from the notorious negative transfer issue so that the model adapted from the pre-trained model (i.e., adapted model) underperforms the model learned from scratch (i.e., ground-built model) in the target task. In this paper, we develop a method, denoted as ANT, to address the negative transfer issue in transferable sequential recommendation. In order to effectively learn more transferable knowledge from auxiliary tasks, ANT not only utilizes item texts but also incorporates item images and prices. As will be shown in our analysis (Section 6.3), item images and prices exhibit better transferability over item texts across tasks. ANT also employs a re-learning-based strategy to better capture the task-specific knowledge in the target task. Specifically, instead of fine-tuning, ANT relearns certain parameters in the pre-trained model during adaptation to enable a more task-specific model in the target task.

We conduct a comprehensive evaluation to compare ANT against eight state-of-the-art baseline methods in five

- Bo Peng is with the Department of Computer Science and Engineering, The Ohio State University, Columbus, OH, 43210.
E-mail: peng.707@buckeyemail.osu.edu
- Srinivasan Parthasarathy is with the Department of Computer Science and Engineering, and the Translational Data Analytics Institute, The Ohio State University, Columbus, OH, 43210.
E-mail: srini@cse.ohio-state.edu
- Xia Ning is with the Department of Biomedical Informatics, the Department of Computer Science and Engineering, and the Translational Data Analytics Institute, The Ohio State University, Columbus, OH, 43210.
E-mail: ning.104@osu.edu
- *Corresponding author

paper received April 19, 2005; revised August 26, 2015.

target tasks. Our experimental results demonstrate that ANT does not suffer from the negative transfer issue on any of the five target tasks. The results also demonstrate that in the five target tasks, ANT significantly outperforms baseline methods, with an improvement of up to 15.2%. Our ablation study demonstrates that item texts, images and prices all significantly contribute to the recommendation performance of ANT. For better reproducibility, we release the processed data, source code and pre-trained recommendation model in <https://github.com/ninglab/ANT>.

2 RELATED WORK

In the last few years, numerous sequential recommendation methods have been developed, which leverage neural networks (e.g., recurrent neural networks) and attention mechanisms. For example, Hidasi *et al.* [5] developed the first gated recurrent units-based methods to estimate users' preferences in a recurrent manner. Nguyen *et al.* [6] developed a neural personalized embedding model (NPE) in which multilayer perceptrons are utilized to capture the non-linear relations among items. Recently, self-attention mechanisms have also been largely employed in developing sequential recommendation methods. Kang *et al.* [7] developed the first self-attention-based sequential recommendation method SASRec, which stacks multiple self-attention layers to estimate users' preferences in an iterative manner. Inspired by SASRec, Sun *et al.* [8] further utilized the cloze objective [9] to enable a self-attention-based bidirectional sequence encoder to better capture users' preferences. Zhang *et al.* [10] developed FDSA in which two self-attention networks are employed to capture the dynamics among items and item texts. Zhou *et al.* [11] developed a self-supervised attentive method S3-Rec in which the mutual information between item embeddings and item attribute embeddings are maximized to enable more expressive representations. Liu *et al.* [12] developed NOVA, a non-invasive self-attentive model to fuse multi-modality item information for better recommendation. Rashed *et al.* [13] developed SASRec++ which integrates multi-modality item information (e.g., texts and images) to improve the performance of SASRec.

To deal with the limited user interaction data in single recommendation tasks, recently, transfer-learning-based sequential recommendation methods are developed to transfer knowledge from auxiliary tasks to the target task for better recommendations. Li *et al.* [14] developed RecGURU, which utilizes a self-attentive autoencoder to generate transferable user representations recommendation. Ding *et al.* [4] developed ZESRec, which utilizes item text embeddings from pre-trained language models as transferable representations of items, and employed the pre-training and fine-tuning framework to transfer knowledge across tasks. Similarly to ZESRec, Hou *et al.* [3] also leveraged item text embeddings as transferable item representations and developed UniSRec. However, different from that in ZESRec, in UniSRec, an embedding transformation module is included to transform the text embeddings and optimize the recommendation performance in the target task.

3 DEFINITIONS AND NOTATIONS

In this paper, we denote a single item as v . For the i -th item v_i , we represent its text, image and price as v_i^t , v_i^m and v_i^p , respectively. We denote a user as u . For the j -th user u_j in a task, we denote her/his historical interactions as a sequence $S_j = \{v_{s_1}(j), v_{s_2}(j), \dots\}$, where $v_{s_t}(j)$ is the t -th interacted item in S_j . Given S_j , the next item that u_j will interact with is referred to as the ground-truth next item, denoted as v_{g_j} . The goal of ANT is to correctly recommend v_{g_j} for u_j . When no ambiguity arises, we will eliminate j in S_j , $v_{s_t}(j)$ and v_{g_j} . We list the key definitions used in this paper as follows:

- Recommendation task: We consider recommending items within a single category as a recommendation task (e.g., movie recommendation, clothes recommendation), following the literature [3], [4], [14]. This is because users could exhibit different behavior patterns in interacting items of different categories.
- Target task: The recommendation task of interest is referred to as the target task, denoted as T^* . We denote the set of all the items in T^* as \mathcal{V}^* .
- Auxiliary task: The recommendation task used to learn transferable knowledge is referred to as an auxiliary task, denoted as T . We denote the set of all the auxiliary tasks as $\mathcal{A} = \{T_1, T_2, \dots\}$, and the set of all the items in the k -th auxiliary task T_k as \mathcal{V}_k .
- User intent modeling: we consider the process of estimating users' preferences via their interacted items as user intent modeling following [15].

We denote matrices, scalars and row vectors using uppercase, lowercase, and bold lowercase letters, respectively.

4 METHOD

Figure 1 presents the ANT architecture, and the pre-training, adaptation and recommendation processes in ANT. ANT transfers knowledge from auxiliary tasks to the target task via pre-training and adaptation. In particular, we pre-train ANT on auxiliary tasks to capture transferable knowledge for recommendations. We assume such knowledge is applicable to the target task, and thus, adapt the pre-trained model to the target task to improve the recommendation performance. To address the negative transfer issue, ANT utilizes item texts, images and prices together to learn more transferable knowledge from auxiliary tasks. In addition, ANT employs a re-learning-based adaptation strategy to enable a more task-specific model in the target task. In what follows, we first present the item representation learning and user intent modeling in ANT in Section 4.1 and Section 4.2, respectively. Then, we present the pre-training process in ANT in Section 4.3 and the adaptation strategy in ANT in Section 4.4.

4.1 Item Representation Learning (IRL)

Existing methods [3], [4] learn item representations using only item texts. However, as will be shown in our own analysis (Section 6.3), the styles, vocabularies and wording of item texts in auxiliary tasks and the target task could be significantly different. Consequently, based exclusively on item texts, we may learn limited transferable knowledge from auxiliary tasks. In order to capture more transferable

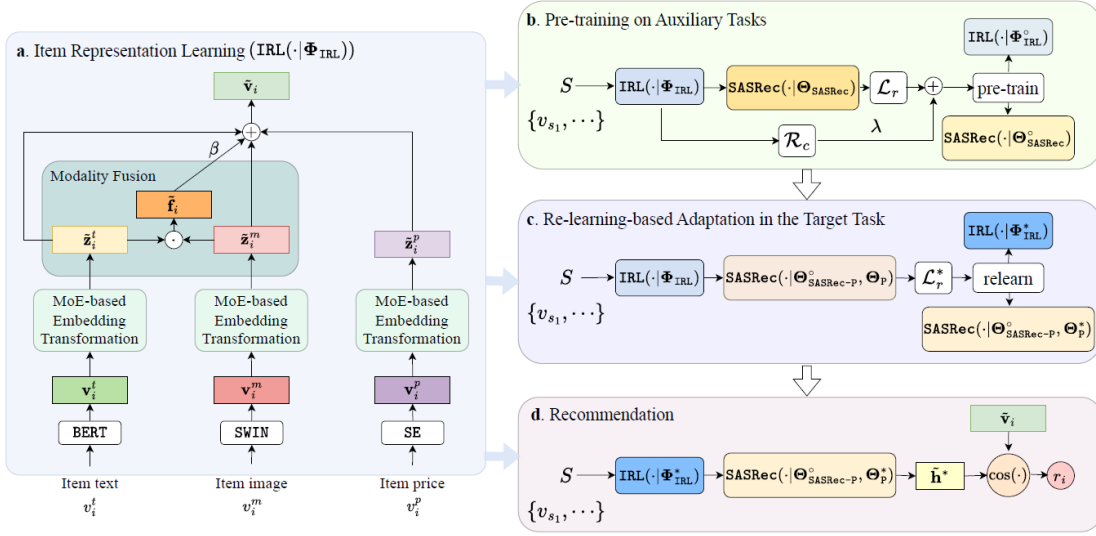


Fig. 1: ANT Model Architecture. Fig. 1a: ANT utilizes item texts, images and prices together to generate item embeddings; Fig. 1b: ANT pre-trains the parameters in IRL (i.e., $\Phi_{\text{IRL}}^{\circ}$) and the user intent model (i.e., $\Theta_{\text{SASRec}}^{\circ}$) to learn transferable knowledge from auxiliary tasks; Fig. 1c: ANT relearns the parameters in IRL (i.e., Φ_{IRL}^{*}) and the position embeddings (Θ_{p}^{*}) to capture the task-specific knowledge in the target task; Fig. 1d: ANT generates recommendations using pre-trained and relearned parameters.

knowledge, in ANT, besides item texts, we also incorporate item images and prices when generating item representations. Specifically, in ANT, we utilize a fixed pre-trained language model (e.g., BERT), a fixed pre-trained vision model (e.g., SWIN) and the sinusoidal encoding (SE), all of which are recommendation-independent, to generate embeddings from item texts, images and prices, respectively. Then, we transform the generated embeddings to better adapt their semantics for user intent modeling. We fix the pre-trained language model and vision model for better efficiency following the literature [3], [4].

4.1.1 Text Embedding Generation

In ANT, we use BERT [9] to generate text embeddings. We also tried other pre-trained language models such as RoBERTa [16] and XLM-RoBERTa [17] but empirically observed that BERT has the best performance. Given the item texts, the pre-trained BERT model downloaded from Hugging Face¹ and the associated tokenizer, we generate the text embeddings as follows:

$$\mathbf{v}_i^t = \text{BERT}(\text{tokenizer}(v_i^t)), \quad (1)$$

where v_i^t and \mathbf{v}_i^t are the text and text embedding of item v_i , respectively.

4.1.2 Image Embedding Generation

In ANT, we utilize SWIN [18] to generate image embeddings since we empirically observed that it outperforms other popular pre-trained vision models such as CLIP [19] and ViT [20]. Particularly, given the item image, the pre-trained SWIN model from Hugging Face and the associated image processor, we generate image embeddings as follows:

$$\mathbf{v}_i^m = \text{SWIN}(\text{processor}(v_i^m)), \quad (2)$$

where v_i^m and \mathbf{v}_i^m are the image and image embedding of item v_i , respectively.

1. <https://huggingface.co/models>

4.1.3 Price Embedding Generation

Embeddings for numerical variables such as prices should be monotonic, transnationally invariant and symmetric in terms of their proximity. As proved in Wang [21], by using an appropriate frequency coefficient, SE [22] could generate embeddings that guarantee the above properties. Therefore, in ANT, we utilize SE to generate price embeddings as follows:

$$\mathbf{v}_i^p = [\dots, \sin(\omega_j v_i^p), \cos(\omega_j v_i^p), \dots], \quad \omega_j = \omega^{-\frac{2j}{d_p}}, \quad (3)$$

where v_i^p and \mathbf{v}_i^p is the price and price embedding of item v_i , respectively; ω_j is the coefficient in the $2j$ and $2j+1$ -th dimension of \mathbf{v}_i^p ; ω is the frequency coefficient in SE, and d_p is the dimension of price embeddings.

4.1.4 Embedding Transformation

We transform embeddings generated from recommendation-independent BERT, SWIN and SE to capture more recommendation-specific information. Particularly, we use the mixture-of-expert (MoE) mechanism for the embedding transformation. During the transformation, we use a projection layer to project the embeddings to spaces that could consist of recommendation-specific information. We consider the projected embeddings as experts and leverage a routing layer to adaptively aggregate the experts to generate transformed embeddings. In ANT, we use parametric whitening [3], [23], [24] for texts and images, and the traditional linear projection for prices.

Parametric Whitening for Texts and Images: Previous study [3] utilizes parametric whitening to project text embeddings and demonstrate superior performance in recommendation tasks. In ANT, we generalize this idea to images and perform the projection of text and image embeddings as follows:

$$\tilde{\mathbf{v}}_i^x(k) = (\mathbf{v}_i^x - \mathbf{b}_k^x) W_k^x, \quad (4)$$

where x denotes the modality, that is $x = t$ or m ; \mathbf{v}_i^x is item v_i 's embedding for modality x ; \mathbf{b}_k^x is a learnable shift parameter for texts or images, and W_k^x is a learnable projection parameter in the k -th projection head, $k \in \{1, 2, \dots, n_h\}$; $\tilde{\mathbf{v}}_i^x(k)$ is the projected embedding from the k -th head.

Linear Projection for Prices: We utilize the widely used linear projection for the transformation of price embeddings as follows:

$$\tilde{\mathbf{v}}_i^p(k) = \mathbf{v}_i^p W_k^p + \mathbf{b}_k^p, \quad (5)$$

where \mathbf{v}_i^p is the price embedding of item v_i , and W_k^p and \mathbf{b}_k^p are learnable parameters in the k -th projection head. We empirically observed that linear projection outperforms parametric whitening for price embeddings.

Aggregation via Gaussian Routing: We learn weights following Gaussian distributions to aggregate the projected embedding $\tilde{\mathbf{v}}_i^x(k)$ ($x = t, m$ or p) for the i -th item as follows:

$$\tilde{\mathbf{z}}_i^x = \text{Softmax}(\boldsymbol{\alpha}_i^x)[\tilde{\mathbf{v}}_i^x(1); \tilde{\mathbf{v}}_i^x(2); \dots; \tilde{\mathbf{v}}_i^x(n_h)], \quad (6)$$

where Softmax is employed to normalize the learned weights

$\boldsymbol{\alpha}_i^x \sim \mathcal{N}(\boldsymbol{\mu}_i^x, \text{diag}((\boldsymbol{\sigma}_i^x)^2))$, and $\tilde{\mathbf{z}}_i^x$ ($x = t, m$ or p) is the transformed embedding of item v_i from modality x . We parameterize the mean $\boldsymbol{\mu}_i^x$ and standard deviation $\boldsymbol{\sigma}_i^x$ of the Gaussian distribution as follows:

$$\boldsymbol{\mu}_i^x = \mathbf{v}_i^x B^x \text{ and } \boldsymbol{\sigma}_i^x = \text{Softplus}(\mathbf{v}_i^x U^x), \quad (7)$$

where B^x ($x = t, m$ or p) and U^x are learnable parameters; Softplus is the activation function to ensure a positive standard deviation. Compared to the widely used linear and cosine [25] routing, the Gaussian routing captures the uncertainty in the weight generation process by modeling it as the variance of the Gaussian distribution, and thus, could improve the model generalizability [26].

4.1.5 Modality Fusion

The synergy among item modalities (e.g., texts and images) have been demonstrated [19] useful for recommendation. For example, with an image of a can and the word ‘‘cat’’ in the text together, we could identify the item as cat can food rather than mistaking it as fish or soda cans based on the item image alone. In ANT, given the transformed text and image embedding $\tilde{\mathbf{z}}_i^t$ and $\tilde{\mathbf{z}}_i^m$ of item v_i , we capture the synergy between the text and image as follows:

$$\tilde{\mathbf{f}}_i = \tilde{\mathbf{z}}_i^t \odot \tilde{\mathbf{z}}_i^m, \quad (8)$$

where $\tilde{\mathbf{f}}_i$ is an embedding representing the synergy between the text and image of item v_i ; \odot is the Hadamard product (i.e., element-wise product). Compared to the widely used Transformer-based approach [27], our Hadamard product-based method is significantly more efficient and could still effectively capture the synergy among the modalities. Note that, item texts and images both reflect intrinsic properties of items (e.g., category, functionality), while item prices could be substantially affected by external factors (e.g., seasonal, festival). Therefore, we only consider synergies between item texts and images, not including prices.

In ANT, we leverage item texts, item images, their synergy and item prices to generate comprehensive item embeddings as follows:

$$\tilde{\mathbf{v}}_i = \text{IRL}(v_i^t, v_i^m, v_i^p | \Phi_{\text{IRL}}, \beta) = \tilde{\mathbf{z}}_i^t + \tilde{\mathbf{z}}_i^m + \tilde{\mathbf{z}}_i^p + \beta \tilde{\mathbf{f}}_i, \quad (9)$$

where $\tilde{\mathbf{v}}_i$ is the comprehensive item embedding of v_i . We introduce a hyper-parameter $\beta \in (0, 1)$ to control the weight of $\tilde{\mathbf{f}}_i$ and mitigate the inflation of common information from text and image into $\tilde{\mathbf{v}}_i$. In Equation 9, Φ_{IRL} is the set of all the learnable parameters for item representation learning:

$$\Phi_{\text{IRL}} = \{\mathbf{b}_k^x, W_k^x, B^x, U^x | x \in \{t, m, p\}, k \in \{1, \dots, n_h\}\}. \quad (10)$$

4.2 User Intent Modeling

Following existing pre-training-based methods [3], [28], in this paper, we utilize the widely used SASRec model for user intent modeling in ANT. However, it should be noted that ANT serves as a general framework that is also compatible with other user intent modeling methods. SASRec is a self-attention-based [22] method, which learns temporal patterns using position embeddings, and stacks multiple self-attention layers to aggregate interacted items and estimate users’ preference in an iterative manner. Specifically, given the interaction sequence $S = \{s_1, s_2, \dots\}$, we stack the embedding of interacted items to generate an embedding matrix for S as follows:

$$M = [\tilde{\mathbf{v}}_{s_1}; \tilde{\mathbf{v}}_{s_2}; \dots], \quad (11)$$

where $\tilde{\mathbf{v}}_{s_i}$ is the embedding of item s_i (Equation 9). With M , we generate the hidden representation of users’ preference $\tilde{\mathbf{h}}$ via SASRec:

$$\tilde{\mathbf{h}} = \text{SASRec}(M | \Theta_{\text{SASRec-P}}, \Theta_{\text{P}}), \quad (12)$$

where $\Theta_{\text{SASRec-P}}$ represents all the learnable parameters in SASRec excluding the position embeddings, and Θ_{P} represents all the learnable parameters in position embeddings. We use SASRec for the user intent modeling in both pre-training on auxiliary tasks (Section 4.3) and adaptation in the target task (Section 4.4).

4.3 Pre-training on Auxiliary Tasks

The user interaction data in the target task (i.e., movie recommendation) is generally sparse. The sparse data may not carry enough information to enable effective recommendation models. To leverage richer data from many auxiliary tasks, in ANT, we learn and transfer knowledge from auxiliary tasks to the target task to improve the recommendation performance in the target task. Particularly, motivated by the success of model pre-training in transfer learning [9], [18], [19], we pre-train a recommendation model on auxiliary tasks. In this Section, we present the loss function and regularization used in our pre-training in detail.

4.3.1 Item Recommendation Loss

We introduce an item recommendation loss in pre-training to learn a pre-trained model from all the auxiliary tasks. We define the negative log likelihood of correctly recommending the next item as the recommendation loss as follows:

$$\mathcal{L}_r = - \sum_{T_k \in \mathcal{A}} \sum_{(S_j, v_{g_j}) \in T_k} \log(p_j), \quad (13)$$

$$\text{where } p_j = \frac{\exp(\cos(\tilde{\mathbf{h}}_j, \tilde{\mathbf{v}}_{g_j})/\tau)}{\sum_{v_{i'} \in \cup_{\mathcal{V}_k} \exp(\cos(\tilde{\mathbf{h}}_j, \tilde{\mathbf{v}}_{i'})/\tau)},$$

where v_{g_j} is the ground-truth next item of the j -th user's interest in an auxiliary task; p_j is the probability of correctly recommending v_{g_j} ; \mathbf{h}_j is the preference of the j -th user in an auxiliary task following SASRec (Equation 12); $\tilde{\mathbf{v}}_{g_j}$ is the embedding of v_{g_j} (Equation 9); \mathcal{V}_k is the set of all the items in the k -th auxiliary task; $\cup \mathcal{V}_k$ is the union of items in all the auxiliary tasks; $\cos(\cdot)$ is the cosine similarity.

4.3.2 Text-image Alignment Regularization

Inspired by CLIP [19], we introduce a text-image alignment regularization to capture the potential complementarity between texts and images. Specifically, given the set of all the items in auxiliary tasks (i.e., $\cup \mathcal{V}_k$), we formulate the text-image alignment regularization using a negative log likelihood as:

$$\mathcal{R}_c = - \sum_{v_i \in \cup \mathcal{V}_k} \log(q_i), \quad (14)$$

where $q_i = \frac{\exp(\cos(\tilde{\mathbf{z}}_i^m, \tilde{\mathbf{z}}_i^t)/\tau)}{\sum_{v_{i'} \in \cup \mathcal{V}_k} \exp(\cos(\tilde{\mathbf{z}}_i^m, \tilde{\mathbf{z}}_{i'}^t)/\tau)}$,

where q_i is the probability of v_i 's text and image carrying the same information; $\tilde{\mathbf{z}}_i^t$ and $\tilde{\mathbf{z}}_i^m$ is the transformed embedding of the text and image of item v_i , respectively (Equation 6); $\tau \in [0, 1]$ is a hyper-parameter to scale the similarities.

4.3.3 Pre-training

Using all the interactions in all the auxiliary tasks, we pre-train the model from auxiliary tasks and optimize the parameters in ANT as follows:

$$(\Phi_{\text{IRL}}^\circ, \Theta_{\text{SASRec}}^\circ) = \underset{\Phi_{\text{IRL}}, \Theta_{\text{SASRec}}}{\operatorname{argmin}} \mathcal{L}_r + \lambda \mathcal{R}_c, \quad (15)$$

where $\mathcal{L}_r + \lambda \mathcal{R}_c = - \sum_{T_k \in \mathcal{A}} \sum_{(S_j, g_j) \in T_k} \log(p_j) - \lambda \sum_{v_i \in \cup \mathcal{V}_k} \log(q_i)$,

where Φ_{IRL}° (Equation 10) is the set of pre-trained parameters for item representation learning that generates $\tilde{\mathbf{v}}_i^x$ (Equation 9); $\Theta_{\text{SASRec}}^\circ = \{\Theta_{\text{SASRec-P}}^\circ, \Theta_{\text{P}}^\circ\}$ is the set of pre-trained parameters in user intent modeling that generates \mathbf{h} (Equation 12); λ is the coefficient for the regularization. We set λ as $1e-3$ in our pre-training for simplicity.

4.4 Re-learning-based Adaptation in the Target Task

Existing work [3], [4] fine-tunes the pre-trained model within the target task to capture target-task-specific knowledge. However, the pre-trained model captures general knowledge from all the auxiliary tasks. Directly fine-tuning the pre-trained model may end up with a local optimum that is not specific enough to capture the unique user behavior patterns in the target task. To address this issue, we develop a re-learning-based adaptation strategy in which instead of fine-tuning, we relearn the parameters for item representation learning in Φ_{IRL} (Equation 10) from scratch in the target task. Intuitively, different tasks require prioritizing different item properties for effective recommendation (e.g., styles in clothes recommendation, casting in movie recommendation). To this end, highly task-specific parameters are desired for item representation learning. In addition, we also relearn the position embeddings in Θ_{P} (Equation 12) to capture the unique temporal patterns in the target task. Compared to fine-tuned parameters, the relearned ones are more

specific to the target task, and thus, could better capture the task-specific knowledge desired. During adaptation, we also fix pre-trained parameters in user intent modeling $\Theta_{\text{SASRec-P}}^\circ$ since we empirically found that updating these parameters does not benefit the recommendation performance in the target task. Note that, although we relearn Φ_{IRL} in the target task, we still implicitly use Φ_{IRL}° during adaptation because they are used in $\Theta_{\text{SASRec-P}}^\circ$. In summary, during adaptation, ANT relearns the parameters in Φ_{IRL} and Θ_{P} to capture the target-task-specific knowledge, while ANT fixes the pre-trained parameters in $\Theta_{\text{SASRec-P}}^\circ$ to leverage the transferable knowledge learned from auxiliary tasks.

ANT Training in the Target Task: We relearn ANT in the target task by minimizing the negative log likelihood of correctly recommending the next item in the target task as follows:

$$\min_{\Phi_{\text{IRL}}^*, \Theta_{\text{P}}^*} \mathcal{L}_r^* = - \sum_{(S_j, v_{g_j}) \in T^*} \log(p_j^*), \quad (16)$$

where $p_j^* = \frac{\exp(\cos(\tilde{\mathbf{h}}_j^*, \tilde{\mathbf{v}}_{g_j}^*)/\tau)}{\sum_{v_{i'} \in \mathcal{V}^*} \exp(\cos(\tilde{\mathbf{h}}_j^*, \tilde{\mathbf{v}}_{i'}^*)/\tau)}$,

$$\tilde{\mathbf{v}}_{i'}^* = \text{IRL}(v_{i'}^t, v_{i'}^m, v_{i'}^p | \Phi_{\text{IRL}}^*),$$

$$\tilde{\mathbf{h}}^* = \text{SASRec}(M^* | \Theta_{\text{SASRec-P}}^\circ, \Theta_{\text{P}}^*),$$

where T^* is the target task; \mathcal{V}^* is the set of all the items in the target task; $\tilde{\mathbf{v}}_{i'}^*$ is the embedding of $v_{i'}$ in the target task; $\tilde{\mathbf{h}}_j^*$ is the preference of the j -th user in the target task; M^* is a matrix containing embeddings of the interacted items in S_j (Equation 11). As shown in Equation 16, during adaptation, we relearn the parameters for item representation learning (i.e., Φ_{IRL}^*), and temporal patterns modeling (i.e., Θ_{P}^*) while fixing pre-trained parameters in $\Theta_{\text{SASRec-P}}^\circ$ (Equation 12). We also fix BERT and SWIN (Section 4.1) during adaptation for better efficiency. After re-learning, for each user in the target task, we calculate the recommendation score of item v_i as follows:

$$r_i = \cos(\tilde{\mathbf{h}}^*, \tilde{\mathbf{v}}_i^*), \quad (17)$$

where r_i is the recommendation score of item v_i . We recommend the top- k items of the highest recommendation scores.

ANT with Interaction-based Item Embedding (ANT_e): During adaptation, we also develop an ANT variant, denoted as ANT_e, in which in addition to embeddings from item modalities (i.e., texts, images and prices), we learn another embedding $\tilde{\mathbf{e}}_i^*$ from user interactions for each item in the target task to generate target-task-specific item representations. Thus, item embeddings in ANT_e are as follows:

$$\tilde{\mathbf{v}}_i^* = \text{IRL}(v_i^t, v_i^m, v_i^p | \Phi_{\text{IRL}}^*) + \tilde{\mathbf{e}}_i^*. \quad (18)$$

In ANT_e, we minimize \mathcal{L}_r^* in terms of the interaction-based item embeddings, Φ_{IRL}^* and Θ_{P}^* as follows:

$$\min_{\Phi_{\text{IRL}}^*, E^*, \Theta_{\text{P}}^*} \mathcal{L}_r^*, \quad (19)$$

where $E^* = [\tilde{\mathbf{e}}_1^*; \tilde{\mathbf{e}}_2^*; \dots]$ is a matrix containing the interaction-based embeddings for all the items in the target task.

5 EXPERIMENTAL SETUP

5.1 Baseline Methods

In our experiment, we compare ANT with three state-of-the-art interaction-based baseline methods that generate item embeddings using only user interactions in the target task: 1) NPE [6] uses neural networks to capture the non-linear relations among items; 2) SASRec [7] estimates users’ intent by leveraging the self-attention mechanisms; 3) BERT4Rec [8] captures users’ preferences using a bidirectional self-attention-based sequence encoder.

In addition, we compare ANT with three state-of-the-art text-based baseline methods that generate item embeddings based on item texts, and user interactions: 1) FDSA [10] uses two self-attention networks to capture the transitions among items, and the transitions among item texts; 2) S3-Rec [11] learns expressive item representations by maximizing the mutual information between the embedding of items and item texts. 3) UniSRec [3] uses item texts to transfer knowledge across recommendation tasks. Note that, UniSRec is a pre-training-based method, and it has been demonstrated superior performance over all the other pre-training-based sequential recommendation methods such as RecGURU [14] and ZESRec [4] by a significant margin. Thus, we include UniSRec for comparison instead of the methods that UniSRec outperforms.

We also compare ANT with the state-of-the-art multi-modality-based method NOVA [12] and SASRec++ [13], which leverage fusion operators to integrate item information from modalities. Compared to NOVA and SASRec++, ANT leverages pre-training and adaptation to transfer knowledge across tasks.

For all the baseline methods except for SASRec++ and NOVA, we use the implementation in RecBole², a widely used library to benchmark recommendation methods. For SASRec++, In the original paper, only item texts and images are used. To enable a fair comparison, we reimplement SASRec++ with PyTorch-Lighting³ to incorporate item prices. We also implement NOVA since its implementation is not publicly available. We use the same evaluation setting (Section 5.3) and the same datasets for target tasks (Section 5.2) in ANT and all the baseline methods. We also use the same text, image and price embeddings in ANT and all the baseline methods if applicable.

We tune the hyper-parameters in ANT and all the baseline methods using grid search. We use the same search range as reported in Hou *et al.* [3] to tune the hyper-parameters for the baseline methods. We report the search ranges for each hyper-parameter, and other important implementation details in the Appendix.

5.2 Datasets

In our experiments, we consider four auxiliary tasks of recommending items of the category food, movie, home and clothing for pre-training, and leverage the Amazon-Food (Food), Amazon-Movies (Movies), Amazon-Home (Home) and Amazon-Clothing (Clothing) datasets for the four tasks. We select these four auxiliary tasks for pre-training because they

TABLE 1: Dataset Statistics

task	dataset	#users	#items	#intrns	#intrns/u	#u/i
Auxiliary	Food	115,349	39,670	1,027,413	8.9	25.9
	Movies	281,700	59,203	3,226,731	11.5	54.5
	Home	731,913	185,552	6,451,926	8.8	34.8
	Clothing	1,164,752	372,593	10,714,172	9.2	28.8
Target	Scientific	8,442	4,385	59,427	7.0	13.6
	Pantry	13,101	4,898	126,962	9.7	25.9
	Instruments	24,962	9,964	208,926	8.4	21.0
	Arts	45,486	21,019	395,150	8.7	18.8
	Office	87,346	25,986	684,837	7.8	26.4

In this table, the column “task” indicates if the datasets are used in auxiliary tasks or target tasks. The column “#users”, “#items” and “#intrns” shows the number of users, items and user-item interactions, respectively. The column “#intrns/u” has the average number of interactions for each user. The column “#u/i” has the average number of interactions for each item.

contain a larger number of user interactions compared to the other tasks, and thus, could have more information for transfer.

In line with UniSRec, we consider five target tasks of recommending items of the category scientific, pantry, instruments, arts and office. We use the Amazon-Scientific (Scientific), Amazon-Pantry (Pantry), Amazon-Instruments (Instruments), Amazon-Arts (Arts) and Amazon-Office (Office) datasets for these target tasks. All of the datasets are from Amazon reviews⁴, which include users’ interactions and reviews on different categories of products. To the best of our knowledge, publicly available datasets from sources other than Amazon reviews do not provide comprehensive item information (e.g., images and prices). Thus, we only utilize datasets from Amazon reviews in our experiments. Following UniSRec, we only keep users and items with at least five interactions and concatenate title, sub-categories and brand of items as the item text. In addition, for each user, we only consider her most recent 50 interactions in the experiments. Table 1 presents the statistics of the processed datasets.

5.3 Experimental Protocol

5.3.1 Training, Validation and Testing Sets

Following the literature [3], [7], [8], for each user, we use her/his last interaction for testing, second last interaction for validation and all the other interactions for training. We tune the hyper-parameters on the validation sets for all methods, and use the best-performing hyper-parameters in terms of Recall@10 as will be discussed below for testing.

5.3.2 Evaluation Metrics

Following the literature [3], [7], [29], [30], we evaluate all the methods using Recall@*k* and NDCG@*k*. We refer the audience of interest to Peng *et al.* [29] for the detailed definitions of both Recall@*k* and NDCG@*k*. In the experiments, we report the average results over all the users for Recall@*k* and NDCG@*k*. We assess the statistical significance of performance differences at these evaluation metrics using the paired t-test.

2. <https://recbole.io/>

3. <https://www.pytorchlightning.ai>

4. <https://jmcauley.ucsd.edu/data/amazon/>

6 EXPERIMENTS AND ANALYSIS

6.1 Overall Performance

Table 2 presents the overall performance of ANT, its variant ANT_e and state-of-the-art baseline methods at $\text{Recall}@k$ and $\text{NDCG}@k$ on the five datasets used for target tasks. In the comparison, we also include a variant of UniSRec, denoted as UniSRec_e . Similarly to ANT_e , UniSRec_e also learns interaction-based item embeddings to enable more task-specific item representations.

As shown in Table 2, overall, ANT_e is the best-performing method on the five datasets. In terms of $\text{Recall}@10$, ANT_e establishes the new state of the art on four out of five datasets (i.e., Scientific, Instruments, Arts and Office), and achieves the second-best performance on Pantry. Similarly, at $\text{Recall}@50$, ANT_e also outperforms all the other methods on four out of five datasets except for Scientific. On average, over the five datasets, ANT_e achieves a remarkable improvement of 6.1% and 2.1% at $\text{Recall}@10$ and $\text{Recall}@50$, respectively, compared to the best-performing baseline method at each dataset. Similarly, in terms of $\text{NDCG}@10$ and $\text{NDCG}@50$, ANT achieves statistically significant improvement over the best-performing baseline method across all the datasets. Table 2 also presents that ANT is the second-best performing method. In terms of both $\text{Recall}@k$ and $\text{NDCG}@k$, ANT achieves the best or second-best performance, and substantially outperforms the baseline methods on all the datasets. For example, in terms of $\text{Recall}@10$, ANT shows a substantial average improvement of 5.1% compared to best-performing baseline methods over the five datasets. These results demonstrate the superior performance of ANT over the state-of-the-art baseline methods.

6.1.1 Comparison between ANT and ANT_e

We notice that as shown in Table 2, without additional interaction-based item embeddings, the performance of ANT is still highly competitive with that of ANT_e . For example, in terms of $\text{Recall}@10$, ANT only slightly underperforms ANT_e by 1.0% averaged over the five datasets. On Pantry, ANT even slightly outperforms ANT_e at $\text{Recall}@10$. These results suggest that with multi-modality information (i.e., texts, images and price) of items, in ANT, we could generate comprehensive item embeddings. As a result, adding interaction-based item embeddings may not provide significant additional information and thus, does not substantially benefit the recommendation performance. To the best of our knowledge, ANT is the first method demonstrating that interaction-based item embeddings are not necessary for the state-of-the-art recommendation performance, if comprehensive item embeddings as those in ANT_e are employed. Note that, compared to ANT_e , without interaction-based item embeddings, ANT could generate recommendations for new items which do not have interactions (i.e., zero-shot recommendation), and thus, would be more practical in real applications.

6.1.2 Comparison between ANT and SASRec

Table 2 presents that ANT achieves superior performance over the best-performing interaction-based method SASRec on all the five datasets. In terms of $\text{Recall}@10$ and $\text{NDCG}@10$, over the five datasets, ANT significantly outperforms SASRec with a remarkable average improvement

of 26.4% and 54.3%, respectively. The primary difference between ANT and SASRec is in two folds: 1) ANT utilizes multi-modality item information to generate comprehensive item embeddings, while SASRec learns item embeddings only using user interactions; 2) ANT leverages the rich interaction data in auxiliary tasks to improve the recommendation performance in the target task via transfer learning, while SASRec learns only from the sparse user interactions in the target task. The substantial improvement of ANT over SASRec indicates the effectiveness of utilizing multi-modality item information and transfer learning for recommendation.

6.1.3 Comparison between ANT and UniSRec_e

As shown in Table 2, ANT also substantially outperforms the best-performing text-based method UniSRec_e at both $\text{Recall}@k$ and $\text{NDCG}@k$. Specifically, compared to UniSRec_e , ANT achieves a remarkable average improvement of 10.2% and 34.9% at $\text{Recall}@10$ and $\text{NDCG}@10$, respectively, over the five datasets. As will be shown in Section 6.3, item texts could be substantially different across tasks. Consequently, based on item texts, UniSRec_e could learn limited transferable knowledge on auxiliary tasks. To address this limitation, ANT also incorporates item images and item prices to more effectively learn transferable knowledge on auxiliary tasks.

6.1.4 Comparison between ANT and SASRec++

Table 2 also shows that ANT could consistently outperform the best-performing multi-modality-based method SASRec++ on all the datasets with substantial improvement (e.g., 5.9% at $\text{Recall}@10$ on Scientific). In ANT, we transfer knowledge from auxiliary tasks to the target task via pre-training and adaptation, while SASRec++ only learns from the information in the target task. The improvement of ANT over SASRec++ suggests the effectiveness of transfer learning in recommendation applications.

6.2 Analysis on Negative Transfer Issue

We conduct an analysis to evaluate if UniSRec, the state-of-the-art pre-training-based method, and ANT suffer from the negative transfer issue. Specifically, in this analysis, we compare the performance of ground-built models (i.e., models learned from scratch) and adapted models (i.e., models adapted from the pre-trained model) of UniSRec and ANT in the target task. We consider two adaptation strategies for learning adapted models: fine-tuning and re-learning in both UniSRec and ANT. During fine-tuning, following that in UniSRec [3], in both UniSRec and ANT, we fix the user intent model and only fine-tune the parameters for item representation learning. For UniSRec, we use the pre-trained model open-sourced by their authors. We denote the ground-built model, the fine-tuned model and the re-learned model as GB, FT and ReL, respectively. We report the performance of GB, FT and ReL from UniSRec and ANT on the five datasets in Table 3.

Table 3 presents that, with fine-tuning, UniSRec substantially suffers from the negative transfer issue. Particularly, the fine-tuned model in UniSRec, denoted as UniSRec-FT , underperforms the model built from scratch, denoted as

TABLE 2: Overall Performance

Dataset	Metric	NPE	SASRec	BERT4Rec	FDSA	S3-Rec	UniSRec	UniSRec _e	NOVA	SASRec++	ANT	ANT _e	imprv (%)
Scientific	Recall@10	0.0772	0.1060	0.0500	0.0907	0.0500	0.1071	0.1163	0.0962	<u>0.1260</u>	0.1334	0.1347	6.9*
	Recall@50	0.1746	0.2022	0.1241	0.1777	0.1315	0.2172	0.2313	0.1761	<u>0.2362</u>	0.2479	0.2460	5.0*
	NDCG@10	0.0375	0.0579	0.0254	0.0588	0.0255	0.0563	0.0613	0.0678	<u>0.0839</u>	0.0864	0.0886	5.6*
	NDCG@50	0.0588	0.0787	0.0414	0.0777	0.0430	0.0802	0.0863	0.0851	<u>0.1079</u>	0.1111	0.1130	4.7*
Pantry	Recall@10	0.0424	0.0537	0.0316	0.0437	0.0462	0.0647	0.0710	0.0536	<u>0.0811</u>	0.0878	0.0864	8.3*
	Recall@50	0.1381	0.1385	0.1000	0.1314	0.1381	0.1719	0.1828	0.1284	<u>0.1886</u>	0.1975	0.1983	5.1*
	NDCG@10	0.0194	0.0235	0.0160	0.0233	0.0226	0.0312	0.0330	0.0288	<u>0.0446</u>	0.0489	0.0485	9.6*
	NDCG@50	0.0400	0.0416	0.0306	0.0420	0.0423	0.0544	0.0571	0.0449	<u>0.0678</u>	0.0727	0.0728	7.4*
Instruments	Recall@10	0.1008	0.1163	0.0821	0.1149	0.1119	0.1115	0.1260	0.1051	<u>0.1276</u>	0.1340	0.1352	6.0*
	Recall@50	0.1984	0.2125	0.1437	0.2116	0.2054	0.2107	<u>0.2418</u>	0.1912	0.2301	0.2404	0.2439	0.9
	NDCG@10	0.0567	0.0673	0.0624	0.0756	0.0668	0.0642	0.0715	0.0766	<u>0.0924</u>	0.0965	0.0969	4.9*
	NDCG@50	0.0778	0.0881	0.0756	0.0964	0.0870	0.0858	0.0967	0.0952	<u>0.1147</u>	0.1196	0.1205	5.1*
Arts	Recall@10	0.0877	0.1122	0.0675	0.1034	0.1017	0.1016	<u>0.1278</u>	0.1093	0.1195	0.1329	0.1361	6.5*
	Recall@50	0.1790	0.2041	0.1313	0.1940	0.1929	0.1996	<u>0.2405</u>	0.1941	0.2209	0.2370	0.2408	0.1
	NDCG@10	0.0467	0.0612	0.0433	0.0676	0.0567	0.0568	0.0700	0.0764	<u>0.0814</u>	0.0905	0.0938	15.2*
	NDCG@50	0.0666	0.0810	0.0571	0.0871	0.0765	0.0781	0.0945	0.0947	<u>0.1035</u>	0.1131	0.1166	12.7*
Office	Recall@10	0.0884	0.1186	0.0838	0.1134	0.1127	0.0996	<u>0.1269</u>	0.1106	0.1178	0.1295	0.1326	4.5*
	Recall@50	0.1527	0.1817	0.1237	0.1722	0.1751	0.1676	<u>0.2014</u>	0.1683	0.1852	0.2021	0.2019	0.2
	NDCG@10	0.0502	0.0787	0.0635	0.0878	0.0775	0.0615	0.0800	0.0863	<u>0.0881</u>	0.0969	0.1007	14.3*
	NDCG@50	0.0642	0.0925	0.0722	0.1006	0.0910	0.0763	0.0963	0.0988	<u>0.1028</u>	0.1127	0.1158	12.6*

For each dataset, the best performance is in **bold**, and the best performance among the baseline methods is underlined. The column ‘imprv’ presents the percentage improvement of ANT over the best-performing baseline methods (underlined). The * indicates that the improvement is statistically significant at 90% confidence level.

TABLE 3: Comparison between Adapted and Ground-built Models

Dataset	Metric	UniSRec			ANT		
		GB	FT	ReL	GB	FT	ReL
Scientific	Recall@10	0.1187	0.1071	0.1211	0.1299	0.1340	0.1334
	Recall@50	0.2319	0.2172	0.2421	0.2406	0.2421	0.2479
	NDCG@10	0.0658	0.0563	0.0644	0.0846	0.0871	0.0864
	NDCG@50	0.0905	0.0802	0.0908	0.1086	0.1106	0.1111
Pantry	Recall@10	0.0698	0.0647	0.0711	0.0808	0.0859	0.0878
	Recall@50	0.1765	0.1719	0.1853	0.1933	0.1955	0.1975
	NDCG@10	0.0336	0.0312	0.0339	0.0444	0.0475	0.0489
	NDCG@50	0.0566	0.0544	0.0587	0.0687	0.0712	0.0727
Instruments	Recall@10	0.1217	0.1115	0.1240	0.1305	0.1333	0.1340
	Recall@50	0.2232	0.2107	0.2311	0.2382	0.2356	0.2404
	NDCG@10	0.0729	0.0642	0.0723	0.0933	0.0960	0.0965
	NDCG@50	0.0949	0.0858	0.0955	0.1166	0.1183	0.1196
Arts	Recall@10	0.1106	0.1016	0.1002	0.1284	0.1256	0.1329
	Recall@50	0.2122	0.1996	0.1990	0.2310	0.2282	0.2370
	NDCG@10	0.0641	0.0568	0.0557	0.0879	0.0855	0.0905
	NDCG@50	0.0861	0.0781	0.0772	0.1103	0.1078	0.1131
Office	Recall@10	0.1055	0.0996	0.1037	0.1268	0.1248	0.1295
	Recall@50	0.1711	0.1676	0.1723	0.1982	0.1951	0.2021
	NDCG@10	0.0707	0.0615	0.0649	0.0949	0.0936	0.0969
	NDCG@50	0.0849	0.0763	0.0798	0.1104	0.1089	0.1127

In this table, GB, FT and ReL represents ground-built models, finetuned models and models adapted with our relearning-based strategy, respectively. For each dataset, the best performance in UniSRec and ANT are in **bold**.

UniSRec-GB, by a remarkable margin across all five datasets. For example, at Recall@10, UniSRec-FT substantially underperforms UniSRec-GB by 8.5% averaged over the five datasets. By contrast, as shown in Table 3 ANT, when finetuned, is less susceptible to negative transfer. Specifically, ANT-FT outperforms the ANT-GB on Scientific, Pantry, and Instruments with a considerable average improvement of 3.9% at Recall@10.

Table 3 also presents that our re-learning-based adaptation strategy could substantially mitigate the negative trans-

fer issue. In particular, the relearned model in UniSRec, denoted as UniSRec-ReL, outperforms UniSRec-GB on Scientific, Pantry and Instruments with an average improvement of 1.9% at Recall@10. Similarly, ANT-ReL also consistently outperforms ANT-GB across all five datasets at all the evaluation metrics, and achieves a substantial average improvement of 3.9% at Recall@10 over ANT-GB. These results demonstrate that by incorporating multi-modality item information (Section 4.1) and leveraging re-learning-based adaptation (Section 4.4), ANT could effectively address the negative transfer issue in existing methods.

6.3 Analysis on Transferability

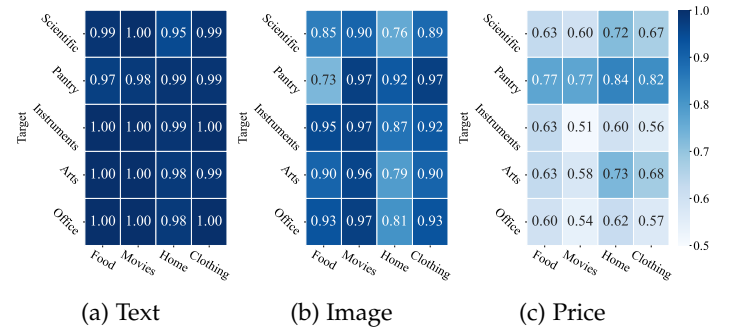


Fig. 2: Task Prediction Accuracy

We conduct an analysis to investigate the cross-task transferability of item texts, images and prices. Intuitively, for each of the item modalities (e.g., text), we could assess its cross-task transferability using the task sensitivity of the modality embeddings (e.g., text embeddings). The higher task sensitivity of the embeddings indicates lower cross-task transferability of the item modality. Previous study [31] indicates that if the embeddings are task-sensitive, a classifier should be able to accurately separate the embeddings from different tasks. Therefore, in this analysis, we measure

the transferability of item texts, images and prices using the cross-task separability of their embeddings.

Particularly, in this analysis, for each target task, we pair it with each of the four auxiliary tasks as in Table 1. For each of the pairs, given the embeddings of a certain item modality (e.g., texts, images and prices), we learn a linear binary classifier to separate the items in the target task from those in the auxiliary task. We use the linear classifier since it has been widely used in studying the separability of embeddings [31], [32]. To enable a balanced classification, for each item in the target task, we uniformly sample one item from the auxiliary task. For items used for classification, we uniformly sample 70%, 10% and 20% for training, validation and testing, respectively. We use the accuracy on the validation set to select the best number of training epochs.

In this analysis, we use the transformed embedding \tilde{z}_i^t , \tilde{z}_i^m and \tilde{z}_i^p (Equation 6) to represent the text, image and price of item v_i . Given embeddings from a certain modality (e.g., text), we measure the cross-task separability of the embeddings using the accuracy of correctly predicting the task which has the corresponding items. A higher accuracy indicates better separability, and thus lower cross-task transferability.

Figure 2a, 2b and 2c shows the classification accuracy on each pair of tasks with text, image and price embeddings, respectively. As shown in Figure 2, text embeddings lead to the highest classification accuracy. Specifically, with text embeddings, using simple linear classifiers, we could achieve accuracies of at least 0.95 on all the pairs indicating that the item texts in target tasks and auxiliary tasks could be significantly different. Thus, item texts could suffer from limited cross-task transferability. Figure 2 also shows that compared to text embeddings, the embeddings of item images and prices are less separable across tasks. For example, in terms of item images, the classification accuracy on the pair (Pantry, Food) is 0.73 implying that items in Pantry and Food could have similar images. Thus, knowledge transfer across the two tasks could be enabled via item images. A similar trend could also be observed with item prices. For item images and item prices, we also tried non-linear classifiers such as two-layer perceptrons but still get similar results (e.g., 0.78 on (Pantry, Food) with item image). These results suggest that item images and prices exhibit stronger cross-task transferability compared to item texts. Therefore, by incorporating them, ANT could more effectively learn transferable knowledge on auxiliary tasks compared to existing pre-training-based methods.

6.4 Ablation Study

We conduct an ablation study to investigate the contribution of item texts, item images, item prices, MoE-based embedding transformation and modality fusion for the recommendation performance in ANT. Specifically, to investigate the contribution of item texts, images and prices, we replace the text, image and price embeddings with zero vectors during the adaptation. To investigate the contribution of MoE-based embedding transformation, we replace our MoE-based approach with simple linear projections for the transformation of text, image and price embeddings. We

TABLE 4: Ablation Study

Dataset	Metric	ANT-T	ANT-I	ANT-P	ANT-MoE	ANT-MF	ANT
Scientific	Recall@10	0.1001	0.1253	0.1314	0.1288	0.1334	0.1334
	Recall@50	0.2000	0.2354	0.2510	0.2473	0.2441	0.2479
	NDCG@10	0.0649	0.0813	0.0855	0.0840	0.0871	0.0864
	NDCG@50	0.0866	0.1051	0.1115	0.1097	0.1112	0.1111
Pantry	Recall@10	0.0839	0.0776	0.0781	0.0845	0.0861	0.0878
	Recall@50	0.1856	0.1875	0.1851	0.1991	0.1965	0.1975
	NDCG@10	0.0468	0.0425	0.0424	0.0473	0.0488	0.0489
	NDCG@50	0.0688	0.0665	0.0654	0.0719	0.0727	0.0727
Instruments	Recall@10	0.1245	0.1222	0.1302	0.1294	0.1336	0.1340
	Recall@50	0.2127	0.2193	0.2366	0.2345	0.2379	0.2404
	NDCG@10	0.0898	0.0879	0.0931	0.0941	0.0958	0.0965
	NDCG@50	0.1088	0.1089	0.1162	0.1169	0.1184	0.1196
Arts	Recall@10	0.1039	0.1159	0.1261	0.1215	0.1310	0.1329
	Recall@50	0.1785	0.2116	0.2299	0.2229	0.2359	0.2370
	NDCG@10	0.0736	0.0778	0.0860	0.0827	0.0894	0.0905
	NDCG@50	0.0899	0.0987	0.1085	0.1048	0.1123	0.1131
Office	Recall@10	0.1123	0.1053	0.1056	0.1173	0.1262	0.1295
	Recall@50	0.1718	0.1705	0.1699	0.1851	0.1962	0.2021
	NDCG@10	0.0840	0.0772	0.0781	0.0877	0.0948	0.0969
	NDCG@50	0.0969	0.0914	0.0921	0.1024	0.1100	0.1127

In this table, “ANT-T”, “ANT-I”, “ANT-P”, “ANT-MoE” and “ANT-MF” represents ANT without item texts, item images, item prices, MoE and modality fusion respectively. The best performance in each dataset is in bold.

also replace the embeddings modeling the synergy between item texts and images (f_i in Equation 8) with zero vectors to investigate the contribution of modality fusion. We denote the ANT ablative variant without texts, images, prices, MoE-based embedding transformation and modality fusion as ANT-T, ANT-I, ANT-P, ANT-MoE and ANT-MF, respectively, and present their performance in Table 4.

As shown in Table 4, with all the modules, ANT outperforms all of its ablative variants on four out of the five datasets except for Scientific. On Scientific, ANT still achieves the best performance at Recall@10, and the second-best performance at Recall@50 and NDCG@10. Particularly, at Recall@10, over the five datasets, ANT achieves an average improvement of 17.8%, 13.4%, 9.0%, 6.2% and 1.3% compared to ANT-T, ANT-I, ANT-P, ANT-MoE and ANT-MF, respectively. In terms of Recall@50, ANT also substantially outperforms ANT-T, ANT-I, ANT-P, ANT-MoE and ANT-MF with an average improvement of 18.8%, 10.2%, 5.8%, 3.5% and 1.3%, respectively, over the five datasets. A similar trend could also be observed at NDCG@10 and NDCG@50. These results show that item texts, item images, item prices, MoE-based embedding transformation and modality fusion all significantly contribute to the recommendation performance of ANT.

7 CONCLUSION

In this paper, we show that state-of-the-art pre-training-based sequential recommendation methods substantially suffer from the negative transfer issue. To address this issue, we introduce ANT that integrates item texts, images and prices together to effectively learn transferable knowledge on auxiliary tasks. In addition, ANT employs a re-learning-based strategy to better capture the task-specific knowledge in the target task. Our experimental results demonstrate that ANT could remarkably outperform the eight state-of-the-art baseline methods, with an improvement of as much as

15.2% in the five target tasks. Our negative transfer analysis shows that ANT could substantially mitigate the negative transfer issue, and the adapted ANT model outperforms the ground-built one on the five target tasks. Our transferability analysis shows that compared to item texts, item images and prices could carry more transferable knowledge. Our ablation study indicates that item texts, images and prices all substantially contribute to the recommendation performance of ANT.

ACKNOWLEDGMENT

This project was made possible, in part, by support from the National Science Foundation grant nos. IIS-2133650 (X.N.). Any opinions, findings and conclusions or recommendations expressed in this paper are those of the authors and do not necessarily reflect the views of the funding agency.

REFERENCES

- [1] R. He and J. McAuley, "Ups and downs: Modeling the visual evolution of fashion trends with one-class collaborative filtering," in *Proceedings of the 25th International Conference on World Wide Web*, ser. WWW '16. Republic and Canton of Geneva, CHE: International World Wide Web Conferences Steering Committee, 2016, p. 507–517. [Online]. Available: <https://doi.org/10.1145/2872427.2883037>
- [2] F. Belletti, M. Chen, and E. H. Chi, "Quantifying long range dependence in language and user behavior to improve RNNs," in *Proceedings of the 25th ACM SIGKDD International Conference on Knowledge Discovery & Data Mining*, ser. KDD '19. New York, NY, USA: Association for Computing Machinery, 2019, p. 1317–1327. [Online]. Available: <https://doi.org/10.1145/3292500.3330944>
- [3] Y. Hou, S. Mu, W. X. Zhao, Y. Li, B. Ding, and J. rong Wen, "Towards universal sequence representation learning for recommender systems," *Proceedings of the 28th ACM SIGKDD Conference on Knowledge Discovery and Data Mining*, 2022. [Online]. Available: <https://api.semanticscholar.org/CorpusID:249625869>
- [4] H. Ding, Y. Ma, A. Deoras, Y. Wang, and H. Wang, "Zero-shot recommender systems," *arXiv preprint arXiv:2105.08318*, 2021.
- [5] B. Hidasi, A. Karatzoglou, L. Baltrunas, and D. Tikk, "Session-based recommendations with recurrent neural networks," *arXiv preprint arXiv:1511.06939*, 2015.
- [6] T. Nguyen and A. Takasu, "NPE: Neural personalized embedding for collaborative filtering," in *Proceedings of the Twenty-Seventh International Joint Conference on Artificial Intelligence, IJCAI-18*. International Joint Conferences on Artificial Intelligence Organization, 7 2018, pp. 1583–1589. [Online]. Available: <https://doi.org/10.24963/ijcai.2018/219>
- [7] W. Kang and J. McAuley, "Self-attentive sequential recommendation," in *2018 IEEE International Conference on Data Mining (ICDM)*. Los Alamitos, CA, USA: IEEE Computer Society, nov 2018, pp. 197–206. [Online]. Available: <https://doi.ieeecomputersociety.org/10.1109/ICDM.2018.00035>
- [8] F. Sun, J. Liu, J. Wu, C. Pei, X. Lin, W. Ou, and P. Jiang, "BERT4Rec: Sequential recommendation with bidirectional encoder representations from transformer," in *Proceedings of the 28th ACM International Conference on Information and Knowledge Management*, ser. CIKM '19. New York, NY, USA: Association for Computing Machinery, 2019, p. 1441–1450. [Online]. Available: <https://doi.org/10.1145/3357384.3357895>
- [9] J. Devlin, M.-W. Chang, K. Lee, and K. Toutanova, "BERT: Pre-training of deep bidirectional Transformers for language understanding," in *Proceedings of the 2019 Conference of the North American Chapter of the Association for Computational Linguistics: Human Language Technologies, Volume 1 (Long and Short Papers)*. Minneapolis, Minnesota: Association for Computational Linguistics, Jun. 2019, pp. 4171–4186. [Online]. Available: <https://aclanthology.org/N19-1423>
- [10] T. Zhang, P. Zhao, Y. Liu, V. S. Sheng, J. Xu, D. Wang, G. Liu, and X. Zhou, "Feature-level deeper self-attention network for sequential recommendation," in *Proceedings of the Twenty-Eighth International Joint Conference on Artificial Intelligence, IJCAI-19*. International Joint Conferences on Artificial Intelligence Organization, 7 2019, pp. 4320–4326. [Online]. Available: <https://doi.org/10.24963/ijcai.2019/600>
- [11] K. Zhou, H. Wang, W. X. Zhao, Y. Zhu, S. Wang, F. Zhang, Z. Wang, and J.-R. Wen, "S3-rec: Self-supervised learning for sequential recommendation with mutual information maximization," in *Proceedings of the 29th ACM International Conference on Information & Knowledge Management*, ser. CIKM '20. New York, NY, USA: Association for Computing Machinery, 2020, p. 1893–1902. [Online]. Available: <https://doi.org/10.1145/3340531.3411954>
- [12] C. Liu, X. Li, G. Cai, Z. Dong, H. Zhu, and L. Shang, "Non-invasive self-attention for side information fusion in sequential recommendation," in *Proceedings of the AAAI Conference on Artificial Intelligence*, vol. 35, no. 5, 2021, pp. 4249–4256.
- [13] A. Rashed, S. Elsayed, and L. Schmidt-Thieme, "Context and attribute-aware sequential recommendation via cross-attention," in *Proceedings of the 16th ACM Conference on Recommender Systems*, ser. RecSys '22. New York, NY, USA: Association for Computing Machinery, 2022, p. 71–80. [Online]. Available: <https://doi.org/10.1145/3523227.3546777>
- [14] C. Li, M. Zhao, H. Zhang, C. Yu, L. Cheng, G. Shu, B. Kong, and D. Niu, "RecGURU: Adversarial learning of generalized user representations for cross-domain recommendation," in *Proceedings of the Fifteenth ACM International Conference on Web Search and Data Mining*, ser. WSDM '22. New York, NY, USA: Association for Computing Machinery, 2022, p. 571–581. [Online]. Available: <https://doi.org/10.1145/3488560.3498388>
- [15] B. Chang, A. Karatzoglou, Y. Wang, C. Xu, E. H. Chi, and M. Chen, "Latent user intent modeling for sequential recommenders," in *Companion Proceedings of the ACM Web Conference 2023*, ser. WWW '23 Companion. New York, NY, USA: Association for Computing Machinery, 2023, p. 427–431. [Online]. Available: <https://doi.org/10.1145/3543873.3584641>
- [16] Y. Liu, M. Ott, N. Goyal, J. Du, M. Joshi, D. Chen, O. Levy, M. Lewis, L. Zettlemoyer, and V. Stoyanov, "RoBERTa: A robustly optimized BERT pretraining approach," *arXiv preprint arXiv:1907.11692*, 2019.
- [17] A. Conneau, K. Khandelwal, N. Goyal, V. Chaudhary, G. Wenzek, F. Guzmán, E. Grave, M. Ott, L. Zettlemoyer, and V. Stoyanov, "Unsupervised cross-lingual representation learning at scale," in *Proceedings of the 58th Annual Meeting of the Association for Computational Linguistics*. Online: Association for Computational Linguistics, Jul. 2020, pp. 8440–8451. [Online]. Available: <https://aclanthology.org/2020.acl-main.747>
- [18] Z. Liu, Y. Lin, Y. Cao, H. Hu, Y. Wei, Z. Zhang, S. Lin, and B. Guo, "Swin Transformer: Hierarchical vision Transformer using shifted windows," in *Proceedings of the IEEE/CVF International Conference on Computer Vision (ICCV)*, October 2021, pp. 10 012–10 022.
- [19] A. Radford, J. W. Kim, C. Hallacy, A. Ramesh, G. Goh, S. Agarwal, G. Sastry, A. Askell, P. Mishkin, J. Clark, G. Krueger, and I. Sutskever, "Learning transferable visual models from natural language supervision," in *Proceedings of the 38th International Conference on Machine Learning*, ser. Proceedings of Machine Learning Research, M. Meila and T. Zhang, Eds., vol. 139. PMLR, 18–24 Jul 2021, pp. 8748–8763. [Online]. Available: <https://proceedings.mlr.press/v139/radford21a.html>
- [20] A. Dosovitskiy, L. Beyer, A. Kolesnikov, D. Weissenborn, X. Zhai, T. Unterthiner, M. Dehghani, M. Minderer, G. Heigold, S. Gelly, J. Uszkoreit, and N. Houlsby, "An image is worth 16x16 words: Transformers for image recognition at scale," in *International Conference on Learning Representations*, 2021. [Online]. Available: <https://openreview.net/forum?id=YicbFdNTTy>
- [21] B. Wang, L. Shang, C. Lioma, X. Jiang, H. Yang, Q. Liu, and J. G. Simonsen, "On position embeddings in BERT," in *International Conference on Learning Representations*, 2021. [Online]. Available: <https://openreview.net/forum?id=onxoVA9FxmW>
- [22] A. Vaswani, N. Shazeer, N. Parmar, J. Uszkoreit, L. Jones, A. N. Gomez, L. u. Kaiser, and I. Polosukhin, "Attention is all you need," in *Advances in Neural Information Processing Systems*, I. Guyon, U. V. Luxburg, S. Bengio, H. Wallach, R. Fergus, S. Vishwanathan, and R. Garnett, Eds., vol. 30. Curran Associates, Inc., 2017. [Online]. Available: https://proceedings.neurips.cc/paper_files/paper/2017/file/3f5ee243547dee91fbd053c1c4a845aa-Paper.pdf

- [23] J. Huang, D. Tang, W. Zhong, S. Lu, L. Shou, M. Gong, D. Jiang, and N. Duan, "WhiteningBERT: An easy unsupervised sentence embedding approach," in *Findings of the Association for Computational Linguistics: EMNLP 2021*. Punta Cana, Dominican Republic: Association for Computational Linguistics, Nov. 2021, pp. 238–244. [Online]. Available: <https://aclanthology.org/2021.findings-emnlp.23>
- [24] J. Su, J. Cao, W. Liu, and Y. Ou, "Whitening sentence representations for better semantics and faster retrieval," *arXiv preprint arXiv:2103.15316*, 2021.
- [25] Z. Chi, L. Dong, S. Huang, D. Dai, S. Ma, B. Patra, S. Singhal, P. Bajaj, X. SONG, X.-L. Mao, H. Huang, and F. Wei, "On the representation collapse of sparse mixture of experts," in *Advances in Neural Information Processing Systems*, S. Koyejo, S. Mohamed, A. Agarwal, D. Belgrave, K. Cho, and A. Oh, Eds., vol. 35. Curran Associates, Inc., 2022, pp. 34600–34613. [Online]. Available: https://proceedings.neurips.cc/paper_files/paper/2022/file/df4f371f1f89ec8ba5014b3310578048-Paper-Conference.pdf
- [26] X. Li, Y. Dai, Y. Ge, J. Liu, Y. Shan, and L. DUAN, "Uncertainty modeling for out-of-distribution generalization," in *International Conference on Learning Representations*, 2022. [Online]. Available: <https://openreview.net/forum?id=6HN7LHyzGgC>
- [27] Y. Xie, P. Zhou, and S. Kim, "Decoupled side information fusion for sequential recommendation," in *Proceedings of the 45th International ACM SIGIR Conference on Research and Development in Information Retrieval*, ser. SIGIR '22. New York, NY, USA: Association for Computing Machinery, 2022, p. 1611–1621. [Online]. Available: <https://doi.org/10.1145/3477495.3531963>
- [28] J. Wang, F. Yuan, M. Cheng, J. M. Jose, C. Yu, B. Kong, Z. Wang, B. Hu, and Z. Li, "TransRec: Learning transferable recommendation from mixture-of-modality feedback," *arXiv preprint arXiv:2206.06190*, 2022.
- [29] B. Peng, Z. Ren, S. Parthasarathy, and X. Ning, "HAM: Hybrid associations models for sequential recommendation," *IEEE Transactions on Knowledge and Data Engineering*, vol. 34, no. 10, pp. 4838–4853, 2021.
- [30] Z. Fan, Z. Liu, Y. Wang, A. Wang, Z. Nazari, L. Zheng, H. Peng, and P. S. Yu, "Sequential recommendation via stochastic self-attention," in *Proceedings of the ACM Web Conference 2022*, ser. WWW '22. New York, NY, USA: Association for Computing Machinery, 2022, p. 2036–2047. [Online]. Available: <https://doi.org/10.1145/3485447.3512077>
- [31] K. Saito, K. Watanabe, Y. Ushiku, and T. Harada, "Maximum classifier discrepancy for unsupervised domain adaptation," in *2018 IEEE/CVF Conference on Computer Vision and Pattern Recognition (CVPR)*. Los Alamitos, CA, USA: IEEE Computer Society, jun 2018, pp. 3723–3732. [Online]. Available: <https://doi.ieeecomputersociety.org/10.1109/CVPR.2018.00392>
- [32] Y. Tian, Y. Wang, D. Krishnan, J. B. Tenenbaum, and P. Isola, "Rethinking few-shot image classification: A good embedding is all you need?" in *Computer Vision – ECCV 2020: 16th European Conference, Glasgow, UK, August 23–28, 2020, Proceedings, Part XIV*. Berlin, Heidelberg: Springer-Verlag, 2020, p. 266–282. [Online]. Available: https://doi.org/10.1007/978-3-030-58568-6_16

Bo Peng is a Ph.D. student at the Computer Science and Engineering Department, The Ohio State University. His research interests include machine learning, data mining and their applications in recommender systems and graph mining.

Srinivasan Parthasarathy received his Ph.D. degree from the Department of Computer Science, University of Rochester, Rochester, in 1999. He is currently a Professor at the Computer Science and Engineering Department, The Ohio State University. His research is on high-performance data analytics, graph analytics and network science, and machine learning and database systems.

Xia Ning received her Ph.D. degree from the Department of Computer Science and Engineering, University of Minnesota, Twin Cities, in 2012. She is currently a Professor at the Biomedical Informatics Department, and the Computer Science and Engineering Department, The Ohio State University. Her research is on data mining, machine learning and artificial intelligence with applications in recommender systems, drug discovery and medical informatics.

APPENDIX A

REPRODUCIBILITY

We implement ANT in Python 3.9.13 with PyTorch 1.10.2⁵ and PyTorch Lightning 1.7.7⁶. Following UniSRec and SASRec, we set the number of self-attention layers and the number of attention heads in each layer as 2, and the dimension for item embeddings as 256 for ANT and all the baseline methods if applicable. We also use the cross entropy loss for ANT and all the baseline methods to enable a fair comparison. Following UniSRec, in ANT, we set the scaling hyper-parameters τ (Equation 13) as 0.07; set the number of projection heads in embedding transformation n_h as 8; and use Adam optimizer with learning rate $1e-3$ on all the datasets. In ANT, we also set the dimension of price embeddings d_p as 64; use 50,000 as the frequency coefficient ω (Equation 3); and normalize the item prices to be in the range of $[0, 100]$. Considering the memory limits in GPUs, we use batch optimization during pre-training and adaptation, and set the batch size as 2,048 following UniSRec. For ANT and all the baseline methods, we initialize all the learnable parameters using the default initialization methods in PyTorch. For NOVA and SASRec++, we search the dimension of item embeddings d from $\{64, 128, 256\}$. In ANT, we search the coefficient of modality interaction embeddings β (Equation 9) from $\{0.1, 0.3, 0.5, 0.7\}$. For UniSRec, we use the hyper-parameters reported by the authors in all the datasets. For NPE, SASRec, BERT4Rec, FDSA and S3-Rec, following UniSRec, we search d and the learning rate lr from $\{64, 128, 300\}$ and $\{3e-4, 1e-3, 3e-3, 1e-2\}$, respectively. Table A1 presents the best-performing hyper-parameters in ANT, ANT_e and all the baseline methods except for UniSRec on the five datasets. We refer the audience of interest to the UniSRec’s GitHub⁷ for the hyper-parameters used in UniSRec.

5. <https://pytorch.org/>

6. <https://www.pytorchlightning.ai/>

7. <https://github.com/RUCAIBox/UniSRec>

TABLE A1: Best-performing Hyper-parameters in ANT, ANT_e and Baseline Methods

Dataset	NPE		SASRec		BERT4Rec		FDSA		S3-Rec		NOVA	SASRec++	ANT	ANT _e
	d	lr	d	lr	d	lr	d	lr	d	lr	d	d	β	β
Scientific	300	3e-3	128	1e-3	128	1e-2	64	3e-3	300	3e-3	256	256	0.1	0.1
Pantry	128	3e-3	300	3e-4	300	3e-3	64	1e-3	300	1e-3	256	256	0.3	0.5
Instruments	128	1e-3	300	3e-4	300	3e-4	128	3e-3	300	1e-3	128	256	0.7	0.1
Arts	128	1e-3	300	3e-4	300	3e-4	128	3e-3	300	3e-3	256	256	0.7	0.1
Office	128	1e-3	300	3e-4	300	3e-4	128	1e-3	300	3e-3	128	256	0.5	0.1

This table presents the best-performing hyper-parameters of ANT, ANT_e and all the baseline methods except for UniSRec on the five datasets.